PERGAMON

Deep-Sea Research I 48 (2001) 1821–1845

DEEP-SEA RESEARCH
PART I

www.elsevier.com/locate/dsr

Role of the Agulhas Current in Indian Ocean circulation and associated heat and freshwater fluxes

Harry L. Bryden[a,*], Lisa M. Beal[b]

[a]*James Rennell Division for Ocean Circulation and Climate, Southampton Oceanography Centre, Southampton SO14 3ZH, UK*
[b]*Scripps Institution of Oceanography, La Jolla CA 92093-0230, USA*

Received 9 March 2000; received in revised form 23 October 2000; accepted 23 October 2000

Abstract

A reduced estimate of Agulhas Current transport provides the motivation to examine the sensitivity of Indian Ocean circulation and meridional heat transport to the strength of the western boundary current. The new transport estimate is 70 Sv, much smaller than the previous value of 85 Sv. Consideration of three case studies for a large, medium and small Agulhas Current transport demonstrate that the divergence of heat transport over the Indian Ocean north of 32°S has a sensitivity of 0.08 PW per 10 Sv of Agulhas transport, and freshwater convergence has a sensitivity of 0.03×10^9 kg s^{-1} per 10 Sv of transport. Moreover, a smaller Agulhas Current leads to a better silica balance and a smaller meridional overturning circulation for the Indian Ocean. The mean Agulhas Current transport estimated from time-series current meter measurements is used to constrain the geostrophic transport in the western boundary region in order to re-evaluate the circulation, heat and freshwater transports across 32°S. The Indonesian Throughflow is taken to be 12 Sv at an average temperature of 18°C. The constrained circulation exhibits a vertical–meridional circulation with a net northward flow below 2000 dbar of 10.1 Sv. The heat transport divergence is estimated to be 0.66 PW, the freshwater convergence to be 0.54×10^9 kg s^{-1}, and the silica convergence to be 335 kmol s^{-1}. Meridional transports are separated into barotropic, baroclinic and horizontal components, with each component conserving mass. The barotropic component is strongly dependent on the estimated size of the Indonesian Throughflow. Surprisingly, the baroclinic component depends principally on the large-scale density distribution and is nearly invariant to the size of the overturning circulation. The horizontal heat and freshwater flux components are strongly influenced by the size of the Agulhas Current because it is warmer and saltier than the mid-ocean. The horizontal fluxes of heat and salt penetrate down to 1500 m depth, suggesting that warm and salty Red Sea Water may be involved in converting the intermediate and upper deep waters which enter the Indian Ocean from the Southern Ocean

* Corresponding author. Tel.: + 44-23-80596437; fax: + 44-23-80596204.
E-mail address: h.bryden@soc.soton.ac.uk (H.L. Bryden).

0967-0637/01/$ - see front matter © 2001 Elsevier Science Ltd. All rights reserved.
PII: S0967-0637(00)00111-4

into warmer and saltier waters before they exit in the Agulhas Current. © 2001 Elsevier Science Ltd. All rights reserved.

Keywords: Heat transport; Hydrographic sections; Transoceanic; Meridional oceanic circulation; Western boundary currents; Agulhas current; Indian Ocean circulation; Meridional overturning circulation

1. Introduction

In 1995 we measured the structure and transport of the Agulhas Current using a lowered acoustic Doppler current profiler (LADCP) on a simultaneous CTD section southeast of Port Edward, South Africa (Fig. 1), where the western boundary current for the South Indian Ocean is most closely confined to the African continental slope (Beal and Bryden, 1997). Our geostrophic transport estimate for the Agulhas Current transport using the V-shaped zero velocity reference surface derived from the LADCP velocities is 73 Sv, in close agreement with the direct LADCP transport estimate of 75 Sv (Beal and Bryden, 1999). From year-long current meter measurements of the Agulhas Current discussed below, the long-term averaged transport of the Agulhas Current is about 70 Sv. While large, this transport is substantially less than the Agulhas Current transport of 85 Sv estimated by Toole and Warren (1993) for this same section taken in 1987. The question

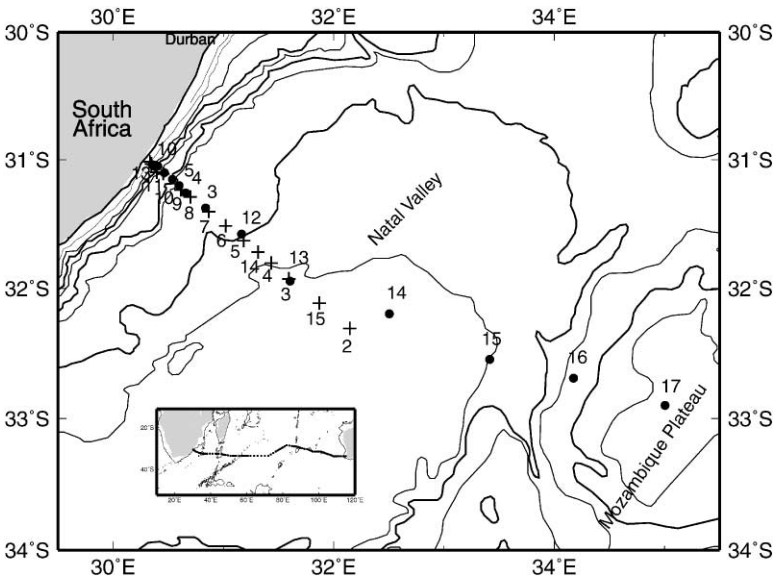

Fig. 1. Hydrographic stations across the Agulhas Current in 1987 (●) and 1995 (+). The 1995 stations aboard RRS *Discovery* include Lowered Acoustic Doppler Current Profiler (LADCP) measurements of velocity at each station. The 1987 stations aboard RRS *Charles Darwin* continued across the Indian Ocean at a nominal latitude of 32°S as shown on the inset. The *Darwin* stations (but not the *Discovery* stations) include silica measurements. Heavier depth contours indicate the 1000, 2000 and 3000 m isobaths.

naturally arises as to how such a different western boundary current transport affects the estimates of Indian Ocean meridional heat and freshwater fluxes and meridional overturning made by Toole and Warren.

We first show that our hydrographic section across the Agulhas Current in 1995 and the 1987 section used by Toole and Warren (1993) have the same baroclinic structure. Next, three cases of large, medium, and small Agulhas Current transports based on plausible reference level choices for the 1987 section across the Agulhas Current are examined to demonstrate the sensitivity of the overall heat flux, freshwater flux, and meridional overturning circulation to the magnitude of the western boundary current. The silica budget is also examined for comparison with Robbins and Toole's (1997) re-analysis of the 32°S section, which utilised a silica budget constraint. We then use the average currents derived from a year-long array of current meter measurements as reference level velocities for our 1995 geostrophic velocity section across the Agulhas Current and join it to the 1987 transindian hydrographic section of Toole and Warren in order to re-evaluate the heat and freshwater fluxes and overturning circulation across 32°S. To help understand the mechanisms of the transports, they are separated into barotropic, baroclinic and horizontal components. The size of the Agulhas Current transport is found to primarily affect the horizontal heat and freshwater transport components.

2. Comparison of the 1987 and 1995 sections across the Agulhas Current

The 1995 CTD/LADCP section aboard RRS *Discovery*, reported by Bryden et al. (1995), followed the same track as the initial part of the 1987 hydrographic section across 32°S aboard RRS *Charles Darwin* reported by Toole and Warren (1993). Both sections extend perpendicularly out from the coast near Port Edward along 130°T to a distance of 160 km, where 1995 station 3 (D3) and 1987 station 13 (CD13) are within 2 km of each other.[1] The 1995 section continued another 60 km out to stations D15 and D2; the 1987 section turned eastward to continue the transindian track along approximately 32°S (Fig. 1).

From the coast to this common point 160 km offshore, the 1987 and 1995 hydrographic sections have similar baroclinic structure. For Toole and Warren's choice of reference level, the geostrophic transport between the coast and CD13 for the 1987 section is -73.0 Sv. With the same pattern of reference levels on the 1995 section, the geostrophic transport out to D3 is -75.8 Sv. The LADCP measurements in 1995, however, suggested a different pattern for the zero velocity surface: a V-shaped reference level extending eastward and downward from the continental slope at 800 m depth to 2900 m at station D6 and then upward out to station D2 at a distance of 230 km from the coast. With this pattern of reference levels, the 1995 geostrophic transport between the coast and station D3 is -66.1 Sv. Utilising a similar spatial pattern for the reference levels on the 1987 section results in a geostrophic transport of -63.3 Sv out to station CD13. The LADCP measurements during the 1995 section clearly showed the Agulhas Undercurrent flowing equatorward on the continental slope beneath the poleward flowing Agulhas Current (Beal and Bryden,

[1] We denote 1987 *Charles Darwin* stations by CD and 1995 *Discovery* stations by D.

1997). From the direct velocity measurements, the Undercurrent transport was estimated to be 6.0 Sv. Using the pattern for the zero-velocity surface suggested by the LADCP section results in a geostrophic transport for the Undercurrent in 1995 of 6.1 Sv and in 1987 of 6.0 Sv. Thus, the baroclinic structures exhibited by the 1987 and 1995 hydrographic sections across the Agulhas current are very similar with a difference in geostrophic transports of less than 3 Sv, or 4%, when a similar reference level scheme is employed for each section.

Thus, the 1987 and 1995 hydrographic sections across the Agulhas Current exhibit nearly identical structure. The difference between Toole and Warren's (1993) transport of 85 Sv for the 1987 section and Beal and Bryden's (1999) transport of 73 Sv for the 1995 section is due to different reference levels, owing to the presence of the Undercurrent. In fact, when Toole and Warren used shipboard ADCP data to reference the 1987 section, they obtained an Agulhas Current transport of 70 Sv; but they then rejected this circulation on the basis of a northward flow of relatively high-salinity Antarctic Intermediate Water which they considered doubtful. Beal and Bryden (1999) showed that the Undercurrent was not inconsistent with southward flowing Red Sea Water and Antarctic Intermediate Water and that most of the northward flowing waters in the Undercurrent are North Atlantic Deep Water. The presence of the Undercurrent reduces the total transport across either the 1987 or 1995 sections by about 15 Sv. Not only does the 6 Sv of equatorward Undercurrent transport take away from net poleward transport, but also the shallower zero-velocity surface means that the upper layer poleward currents are less strong and hence the poleward transport decreases further.

In summary, direct velocity measurements made across the Agulhas Current indicate that the net transport of the Agulhas Current is about 70 Sv, 15 Sv less than the transport estimated by Toole and Warren (1993) primarily because their geostrophic reference level did not resolve the counter-flowing Agulhas Undercurrent. This Undercurrent appears to be a permanent northward flow hugging the continental slope beneath the Agulhas Current (Donohue et al., 2000).

3. Baroclinic structure of the mid-ocean meridional geostrophic circulation

East of the Mozambique Plateau is the mid-ocean expanse of the South Indian Ocean. Toole and Warren's (1993) hydrographic section across the mid-ocean consisted of 93 stations along a nominal latitude of 32°S from station CD17 on the Mozambique Plateau to station CD109 in 50 m water depth on the Australian continental shelf. From this mid-ocean transect, we have estimated geostrophic transports for various choices of the zero velocity surface (Table 1).

First we reproduce Toole and Warren's (1993) circulation. Toole and Warren chose a zero-velocity surface for each station pair after careful consideration of the water mass characteristics and of the bottom topography. In doing so, they emphasised northward flow of the deep water by forcing strong northward bottom velocities where the water mass characteristics suggested an Atlantic or Antarctic source; by downplaying any southward recirculation of the deep waters; and by adjusting bottom triangle transports, which effectively added an extra 4.3 Sv of northward bottom water flow over the mid-ocean section. Overall, Toole and Warren reported a net northward transport below 2000 dbar of 27 Sv, of which approximately 25.6 Sv occurs in the mid-ocean region east of the Mozambique Plateau. We have repeated Toole and Warren's

Table 1
Geostrophic transports for various reference levels[a]

	Mid-ocean section: east of Mozambique Plateau Reference level						Natal valley: west of Mozambique Plateau	
	Toole-Warren (1993)	1800 dbar	2000 dbar	3000 dbar	4000 dbar	Bottom	Toole-Warren reference level	Combined 1995–1987 LADCP reference level
0–1000 dbar	38.5	32.6	32.3	28.3	26.2	28.6	− 67.4	− 59.4
1000–2000 dbar	6.9	1.2	0.9	− 3.2	− 5.2	− 2.8	− 13.5	− 7.2
2000–3000 dbar	7.9	3.4	2.4	− 1.7	− 3.7	− 1.4	+ 1.1	+ 4.2
3000–4000 dbar	10.0	4.2	4.1	1.5	− 0.7	+ 1.6	+ 0.3	+ 1.9
4000–5000 dbar	1.8	1.7	2.2	0.9	− 0.1	+ 0.7		
5000–Bottom	1.2	0.8	1.0	1.0	0.0	+ 0.1		
Total	66.3 (+ 4.3)	43.9	42.9	26.8	16.5	27.4	− 79.5	− 60.5
Transport below 2000 dbar	20.9 (+ 4.3)	10.1	9.7	1.7	− 4.5	1.0	1.4	6.1
Velocity at 2000 dbar	+ 0.101	+ 0.006	0.000	− 0.068	− 0.101	− 0.062		
Transport − v_{2000} × area	39.6	42.3	42.9	44.8	43.2	43.8		

[a] All calculations use 1987 measurements made on board RRS *Charles Darwin* reported by Toole and Warren (1993).

geostrophic transport calculations[2] but using a standard bottom triangle transport calculation (velocity at deepest common level multiplied by bottom triangle area) rather than their complex adjustments, which we do not favour. The result is a net northward transport of 66.3 Sv over the mid-ocean section of which 20.9 Sv occurs below 2000 dbar. Adding the 4.3 Sv of northward flow of bottom water associated with Toole and Warren's bottom adjustments would yield a net mid-ocean deep water flow of order 25 Sv, suggesting that we can reproduce Toole and Warren's circulation, and hence their overturning and heat flux estimates.

To study the baroclinic structure of the mid-ocean circulation, we have also made geostrophic transport estimates using zonally uniform zero-velocity surfaces of 1800, 2000, 3000, 4000 dbar and the bottom (Table 1). The 1800 dbar reference is included because it maximises the northward mid-ocean transport as the zonally averaged baroclinic northward velocity profile exhibits a minimum near 1800 dbar (Fig. 2). In all cases except for the 4000 dbar reference level, there is a net northward flow of deep waters. The size of the deep water flow, however, is 10 Sv or less, much smaller than in the Toole and Warren (1993) circulation. The overall transports for different reference levels can be effectively normalised by subtracting the velocity at 2000 dbar times the cross-sectional area from the overall transport. Normalised transports are all within 2.1 Sv of a net northward transport of 42.7 Sv. Therefore, the baroclinic structure of the circulations for various reference level choices are effectively the same, and normalising the transports collapses the velocity profiles onto that for the choice of zero-velocity surface at 2000 dbar. In terms of the mid-ocean averaged circulation then, the Toole and Warren meridional circulation can be reproduced by using a spatially uniform zero-velocity surface at 2000 dbar and adding a northward flow of $0.10\,\mathrm{cm\,s^{-1}}$ everywhere across the mid-ocean transect. The horizontal structure of such a circulation would be different from Toole and Warren's circulation, however, because Toole and Warren carefully chose the reference surface in regions of deep western boundary currents in an effort to make the strength and direction of the boundary currents match the water mass characteristics.

Knowing the strength of boundary current flows can be useful for constraining the mid-ocean circulation. For example, Bryden and Hall (1980) used the measured Gulf Stream transport through Florida Straits to determine an average reference level velocity for the transatlantic 24°N section and then to calculate meridional heat transport across the entire section. Alternatively, the mid-ocean baroclinic transport can be used as a constraint on an unknown western boundary current transport. Again using a heat transport example, Bryan (1962) used the mid-ocean Sverdrup transport to define the strength of the western boundary current in his estimates of heat transport for the Atlantic and Pacific. Toole and Warren (1993) chose reference levels independently for the western boundary and interior stations and felt justified when the net geostrophic transport across the complete section gave a reasonable value for the combined Ekman transport

[2] Using the pressure of the zero-velocity surface for each station pair described by Toole and Warren (1993) yielded a meridional geostrophic flow that is approximately 10 Sv less northward over the mid-ocean region than the one ultimately used here and ascribed to Toole and Warren. After the discrepancy in transports was noted, Paul Robbins (personal communication) indicated that the reference surfaces described by Toole and Warren's text were in a few cases slightly different from those actually used. The changes were primarily for station pairs 42–43, 45–46, and 101–102. Here we have utilised the revised reference levels provided by Robbins and we believe them to be the ones actually used by Toole and Warren (1993).

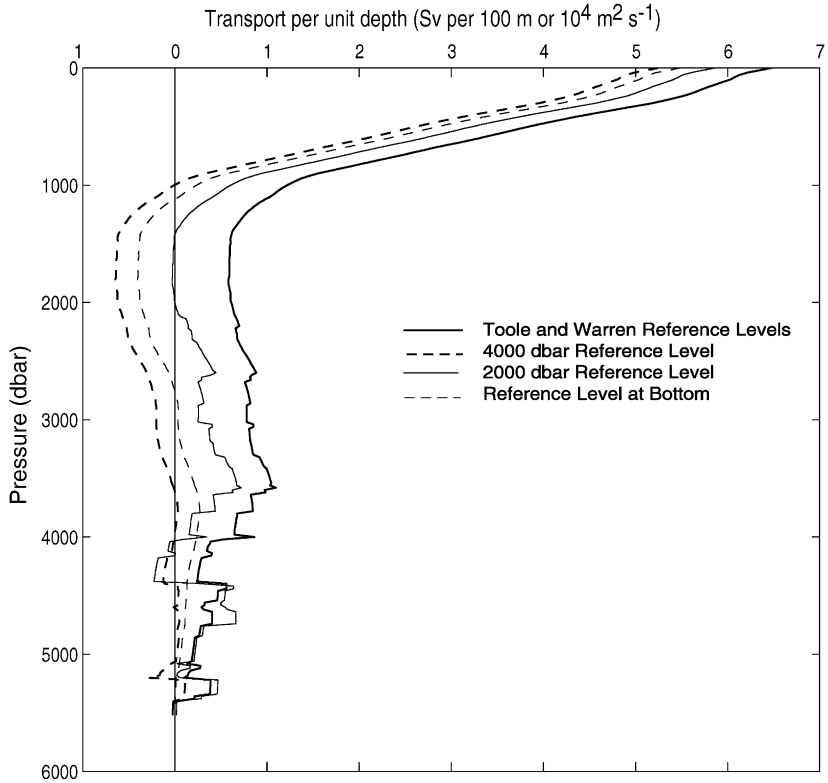

Fig. 2. Baroclinic structure of the zonally averaged mid-ocean northward velocity for various choices of reference level. Transport per unit depth equals the zonally averaged cross-track (positive northward) velocity multiplied by the width of the mid-ocean 32°S section at each pressure level.

and Indonesian Throughflow of 8.3 Sv. Their 85 Sv southward flowing Agulhas Current was balanced by a 77 Sv northward interior flow. As pointed out above, however, the mid-ocean geostrophic transport referenced to a deep horizontal level of no motion is a maximum of 44 Sv for the 32°S transindian section, so substantial deep northward currents are necessary to make the mid-ocean transport more closely match an 85 Sv Agulhas Current. With a smaller Agulhas Current transport of order 70 Sv, which is still larger than the mid-ocean baroclinic transport of 44 Sv, the mid-ocean circulation requires smaller northward velocities in the deep waters. Thus, for smaller Agulhas Current transport we expect a smaller overturning circulation, smaller poleward heat transport divergence and smaller silica transport convergence.

4. Sensitivity

For examining the sensitivity of the overturning circulation and meridional heat flux across 32°S to the size of the Agulhas Current, the constancy in baroclinic structure of the mid-ocean circulation is most useful. If the Agulhas Current transport is substantially less than that estimated

by Toole and Warren (1993) as suggested by direct velocity measurements, the mid-ocean circulation referenced to a 2000 dbar zero-velocity surface can be adjusted by adding or subtracting an appropriate barotropic component, equivalent to a velocity at 2000 dbar, to make the mid-ocean transport match the revised Agulhas Current transport.

For the sensitivity calculations, we use the 1987 transindian hydrographic section exclusively. For the region east of the Mozambique Plateau (beyond station CD17), the basic circulation is taken to be that calculated using a 2000 dbar reference level which yields a net northward flow of 42.2 Sv after adding a small southward bottom triangle transport of 0.7 Sv. For the part of the section across Natal Valley three different reference level schemes are used in order to produce reasonable variations in the transport of the Agulhas Current. First we repeat Toole and Warren's calculations using deep reference levels, 2000 dbar near the continental slope deepening to 2500 and 3000 dbar over the central Natal Valley, to produce a maximum transport for the Agulhas Current of 84.6 Sv and a net southward transport across the Natal Valley section of 79.4 Sv. (All transport values now include bottom triangle transports.) Next, we choose reference levels based on the 1995 LADCP section across the Agulhas Current which exhibited a V-shaped pattern for the zero-velocity surface, deepening from 800 dbar on the continental slope down to 2900 dbar at 60 km from shore and then rising back up to 2000 dbar beyond 100 km from the coast. Such reference levels produce a maximum Agulhas Current transport of 66.3 Sv and a net southward transport across Natal Valley of 60.5 Sv in reasonable agreement with our transport estimates for the 1995 section. Finally, to produce a smaller Agulhas Current transport, we raised the LADCP-indicated reference levels by about 250 dbar between stations CD6, 5, 4, and 3 to reflect a slightly stronger Agulhas Undercurrent as observed in a repeat LADCP survey in April 1996 (Beal, 1997). Such a pattern of reference levels produced a maximum Agulhas Current transport of 55.2 Sv and a net southward transport across the Natal Valley of 50.2 Sv.

To estimate the heat transport[3] for these three sizes of the Agulhas Current (maximum transports of 84.6, 66.3 and 55.2 Sv), we adjust the mid-ocean circulation east of the Mozambique Plateau barotropically and uniformly with a reference level velocity at 2000 dbar to produce a mass balance for the flow across 32°S in each case. For consistency, we maintain Toole and Warren's estimates for the Ekman transport (1.6 Sv northward) and for the Indonesian Throughflow (6.7 Sv) and their temperatures and salinities so that the total southward geostrophic flow across 32°S must be approximately 8.3 Sv.[4] The resulting heat flux divergence over the Indian Ocean north of 32°S is 1.00 PW ($1\,\mathrm{PW} = 1 \times 10^{15}\,\mathrm{W}$) for the large Agulhas transport, 0.84 PW for the intermediate Agulhas transport, and 0.77 PW for the small Agulhas Current transport (Table 2). Thus, we estimate the sensitivity of overall Indian Ocean heat flux estimates to the size of the Agulhas Current to be 0.08 PW per 10 Sv of Agulhas Current transport.

[3] The heat transport calculations are done with the methods described below in the section Mechanisms of Heat and Freshwater Transports.

[4] The net mass transport across 32°S must actually balance the difference between the Throughflow and the net evaporation over the Indian Ocean north of 32°S. The net evaporation is determined by forcing the overall salt flux divergence to be zero. Toole and Warren (1993) estimated the Throughflow transport to be 6.7 Sv and the net evaporation to be $0.48 \times 10^9\,\mathrm{kg\,s^{-1}}$.

Table 2
Sensitivity of circulation to the strength of the Agulhas Current

	Large Agulhas after Toole and Warren (1993)	Medium Agulhas 1995 LADCP reference level	Small Agulhas 1996 LADCP reference level
Transport across Natal valley (Sv)	− 79.4	− 60.5	− 50.2
Maximum transport of Agulhas Current (Sv)	− 84.6	− 66.3	− 55.2
Overturning circulation (Sv)			
Overall Northward transport below 2000 dbar	25.0	20.1	18.6
Through Natal valley	1.4	6.1	9.7
Across Mid-ocean east of Mozambique Plateau	23.5	14.0	8.9
Heat flux (PW)	− 1.00	− 0.84	− 0.77
Freshwater flux ($\times 10^9$ kg s^{-1})	0.52	0.46	0.43
Silica flux (kmol s^{-1})	1802	1332	1039

Ekman transport is taken to be 1.6 Sv at a temperature of 19.4°C, salinity of 35.7;
Indonesian Throughflow transport is taken to be 6.7 Sv at a temperature of 24°C, salinity of 34.5 following Toole and Warren (1993).
Sensitivity to the strength of the Agulhas Current is estimated to be
for heat flux: 0.08 PW per 10 Sv of Agulhas Current transport
for freshwater flux: 0.03×10^9 kg s^{-1} per 10 Sv of Agulhas Current transport
for silica flux: 260 kmol s^{-1} per 10 Sv of Agulhas Current transport

The freshwater convergence for the Indian Ocean north of 32°S also decreases as Agulhas Current transport decreases. For the large Agulhas transport of 84.6 Sv, the net evaporation over the Indian Ocean is estimated to be 0.53×10^9 kg s^{-1}; for the medium Agulhas transport of 66.3 Sv, the net evaporation is reduced to 0.46×10^9 kg s^{-1}; and for the small Agulhas of 55.2 Sv, the net evaporation is 0.43×10^9 kg s^{-1}. Thus, the sensitivity in freshwater convergence is estimated to be 0.03×10^9 kg s^{-1} per 10 Sv of Agulhas Current transport.

The sensitivities in heat and freshwater transports to the size of the Agulhas Current can be understood by examining the average temperatures and salinities of the western boundary region and of the mid-ocean expanse of the Indian Ocean. The average temperature for the Natal Valley of 6.6°C is nearly 2°C warmer than the average mid-ocean temperature of 4.7°C due both to the warmer western boundary current and to the somewhat smaller average depth of the Natal Valley. Similarly, the western boundary region is saltier, as the average salinity in Natal Valley is 0.1 higher than the average mid-ocean salinity. For constant baroclinic structure, an increase of 10 Sv in the poleward flowing current through Natal Valley is compensated by equatorward mid-ocean flow, producing a stronger poleward heat flux of order 0.08 PW ($10\,\text{Sv} \times 2^\circ\text{C} \times 4\,\text{W cm}^{-3}\,\text{C}^{-1}$) and a stronger equatorward freshwater flux of 0.03×10^9 kg s^{-1} ($10\,\text{Sv} \times 0.1/35$).

The size of the meridional overturning for the Indian Ocean circulation is also dependent on the size of the Agulhas Current. The overturning, defined to be the net northward transport below

2000 dbar following Toole and Warren's convention, is 24.9 Sv for the large Agulhas Current reducing to 20.1 Sv for the intermediate Agulhas transport and to 18.6 Sv for the small Agulhas. The size of the Agulhas Current affects the relative contributions of the deep northward flow in the western boundary region and the deep flow in the mid-ocean region to the overturning circulation. For Toole and Warren's circulation, the deep northward flow below 2000 dbar through Natal Valley is only 1.4 Sv while the mid-ocean transport below 2000 dbar is 23.5 Sv. For intermediate and small Agulhas Current transports, the northward flow through the Natal Valley increases due to the equatorward flowing Undercurrent and the deep mid-ocean northward flow decreases because smaller northward reference level velocities are required to provide an overall mass balance to the smaller Agulhas transports. For the intermediate Agulhas transport of 66 Sv, the northward transport below 2000 dbar through Natal Valley is 6.1 Sv and the deep northward mid-ocean transport is 14.0 Sv. But, for the small Agulhas Current transport case, most of the overturning is actually contributed by the northward flow of North Atlantic Deep Water through the Natal Valley section associated with the Agulhas Undercurrent: the deep flow through Natal Valley is 9.7 Sv, while the net mid-ocean northward flow below 2000 dbar is 8.9 Sv (Table 2).

The constancy of the mid-ocean baroclinic circulation also makes estimates of the sensitivity in heat transport to changes in the Ekman transport and Indonesian Throughflow quite straightforward. For these calculations of heat transport, any change in the Ekman transport, which occurs at the mixed layer temperature (effectively the sea-surface temperature), or the Throughflow transport, which Toole and Warren took to have an average temperature of 24°C, is balanced by a barotropic adjustment of the mid-ocean transport at the section-averaged temperature of 4.66°C because the baroclinic structure is taken to be constant. Zeroing or doubling the Ekman transport of 1.6 Sv then changes the overall heat flux divergence over the Indian Ocean by $\pm$ 0.10 PW (1.6 Sv $\times$ [19.58–4.70°C]) for a sensitivity of 0.06 PW per 1 Sv. Zeroing or doubling the Indonesian Throughflow of 6.7 Sv changes the overall heat flux divergence by $\pm$ 0.53 PW (6.7 Sv $\times$ (24–4.70°C)) for a sensitivity of 0.08 PW per 1 Sv change in the Throughflow transport. Clearly, the Indian Ocean heat flux divergence is very sensitive to the size of the Throughflow. The Throughflow carries warm, tropical waters into the Indian Ocean, and these waters must mix substantially before they exit across 32°S where the average surface temperature is less than 20°C. Given the baroclinic structure observed on the 32°S section, a very large Indonesian Throughflow could actually reverse the sign of the overall air–sea heat exchange for the Indian Ocean. We estimate that a Throughflow larger than 17.7 Sv, which is smaller than some estimates for the Throughflow, could actually reverse the sign of the heat flux divergence for the Indian Ocean north of 32°S.

The sensitivity of the freshwater fluxes to changes in Ekman transport and Indonesian Throughflow can also be estimated in a similar manner. Taking an average sea-surface salinity of 35.66 for the Ekman component, Toole and Warren's estimate of 34.5 for the salinity of the Throughflow and the section-averaged salinity of 34.76, zeroing or doubling the Ekman transport of 1.6 Sv changes the overall net evaporation over the Indian Ocean by $\pm\, 0.04 \times 10^9\,\mathrm{kg\,s^{-1}}$ (1.6 Sv $\times$ [35.66–34.76]/34.76) for a sensitivity of $0.03 \times 10^9\,\mathrm{kg\,s^{-1}}$ per 1 Sv of Ekman transport. Zeroing or doubling the Indonesian Throughflow changes the overall net evaporation by $\pm\, 0.05 \times 10^9\,\mathrm{kg\,s^{-1}}$ (6.7 Sv $\times$ [34.5–34.76]/34.76) for a sensitivity of less than $0.01 \times 10^9\,\mathrm{kg\,s^{-1}}$ per 1 Sv of Throughflow transport. Note that this calculation indicates much less sensitivity for the freshwater flux on the Throughflow than the estimates by Robbins and Toole (1997), who argued that any change in Throughflow would be compensated by a change in the higher salinity upper water transport.

While we agree that temporal changes in the Throughflow would likely show up in changes to the upper water circulation, we are considering here that the Throughflow has a mean transport of 6.7 Sv, but with an uncertainty of 6.7 Sv, and that the overall baroclinic structure of the water masses remains constant. Our sensitivity calculation is then an estimate of how errors in the magnitude of the mean Throughflow would affect the freshwater flux across 32°S assuming the 1987 transindian hydrographic section to be representative of the mean baroclinic structure of the circulation. Overall, the estimate of net evaporation over the Indian Ocean north of 32°S is not very sensitive to changes in the Ekman or Throughflow transports; for the Ekman component because the transport is relatively small, and for the Throughflow component because the Throughflow salinity is close to the section-average salinity.

5. Silica considerations

Robbins and Toole (1997) pointed out that Toole and Warren's (1993) circulation across 32°S led to a considerable convergence of silica in the Indian Ocean north of 32°S: deep water flowing northward brings high silica into the Indian Ocean while the compensating southward currents in the thermocline with much lower silica cannot balance the deep input associated with the meridional overturning circulation of order 25 Sv. To prevent a buildup of silica in the Indian Ocean, Robbins and Toole added a silica conservation constraint for the circulation across 32°S and showed that the resulting overturning circulation was reduced by half to about 12 Sv and that the heat flux was also reduced to 0.42 PW. Their consideration of the overall silica budget, however, placed little constraint on the western boundary current transport so that Robbins and Toole's revised circulation made only small changes to the Agulhas Current and their maximum Agulhas Current transport remained above 80 Sv.

To explore what effects the reduced size of the Agulhas Current has on the Indian Ocean silica budget, we used the 1987 measurements to estimate the silica transport across 32°S for the three cases of Agulhas Current transport considered above: a large Agulhas transport of 84.6 Sv based on Toole and Warren's reference levels, an intermediate Agulhas of 66.3 Sv based on reference levels suggested by the 1995 LADCP measurements, and a small Agulhas of 55.2 Sv based loosely on the 1996 LADCP measurements. Assuming zero silica content for the surface Ekman flow and for the Indonesian Throughflow, we found that the large Agulhas led to a silica convergence of 1802 kmol s^{-1}, the intermediate Agulhas to a convergence of 1343 kmol s^{-1}, and the small Agulhas to a convergence of 1152 kmol s^{-1} (Table 2). Thus, the size of the Agulhas has a substantial effect on the silica transport. Indeed, the overall silica transport for the circulation across 32°S based on an Agulhas Current transport determined from observations which include a deep Undercurrent is substantially less than that implied by Toole and Warren's circulation.

There are two reasons for the dependence of silica transport on Agulhas Current transport. First, a smaller Agulhas transport leads to a smaller overturning circulation, as described above, so there is less deep water with high silica flowing equatorward which reduces the northward silica transport. The second reason is that the silica content below 2000 dbar in the Natal Valley is much lower than that in the mid-ocean region, typically 70 μmol kg^{-1} beneath the Agulhas compared with 100–110 μmol kg^{-1} in the interior; smaller Agulhas Current transports are associated with a higher contribution of northward flowing deep waters in the Natal Valley; hence even the deep

northward flow below 2000 dbar in Natal Valley, which contributes to the overturning, has lower silica content and generates a smaller northward silica transport than a comparable deep flow in the interior.

The silica budget for the Indian Ocean north of 32°S is also strongly dependent on the value of the Indonesian Throughflow transport. The Throughflow enters the Indian Ocean with effectively zero silica content. In the procedures used above, any change in Throughflow transport is compensated by flow across 32°S at the section-averaged property value, which for silica is approximately 75 μmol kg^{-1}. Thus, increasing the Throughflow transport from its nominal value of 6.7–12 Sv would reduce the northward silica flux across 32°S, and also the overall convergence of silica north of 32°S, by 5.3 Sv × 75 μmol kg^{-1} = 400 kmol s^{-1}. Changes in Ekman transport may be accounted for in a similar manner so that doubling the Ekman transport from its value of 1.6 Sv would also reduce the silica convergence by 120 kmol s^{-1}.

6. Heat and freshwater fluxes and overturning for the 32°S section

To estimate a definitive circulation and evaluate the fluxes across the transindian 32°S section, we join the 1995 *Discovery* section across the Agulhas Current out to station D2 with the 1987 *Charles Darwin* section beginning with station CD15[5] (Fig. 1). Because silica was not measured on the 1995 hydrographic section, we mapped 1987 silica measurements onto the nearest 1995 stations in order to make silica flux estimates on the joint 1995–1987 transindian section. To determine the circulation, we follow Toole and Warren's (1993) approach of choosing a reference level of zero velocity for each station pair and calculating geostrophic velocities and transports. In the western boundary region, the reference level is guided by direct current measurements. Across the mid-ocean section beyond station D15, we initially choose a constant reference level of 2200 dbar matching the zero-velocity surface from the current meter measurements in the offshore region of the Agulhas Current. Other improvements can be made to the landmark analysis by Toole and Warren (1993). For example, Robbins and Toole (1997) showed the usefulness of considering silica flux to constrain the overall vertical–meridional circulation across 32°S. Here we implement several adjustments to the horizontal structure of the circulation across 32°S to improve the circulation estimate before considering a silica constraint.

The most notable adjustment we make is to the circulation in the western boundary region following the recent measurements of the structure and transport of the Agulhas Current and Undercurrent. Also, adjustment to the eastern boundary region seems justified on the basis of new current meter measurements in the Leeuwin Current. Further, the circulation over Broken Plateau, a relatively shallow feature which the 1987 section followed for 1200 km, is adjusted so that the equatorward transport over the Plateau equals the Sverdrup transport derived from wind climatologies. Finally, new measurements of the Indonesian Throughflow suggest that its transport into

[5] While we considered joining the two sections at the common position of D3 and CD13, we preferred to use the reference velocity information from the 1995–96 current measurements which followed the track out D2; and we also considered joining station D2 to station CD14 but the resulting zigzag track was unappealing while the transports were very similar to just joining with station CD15.

the Indian Ocean is somewhat larger, of order 12 Sv, and its representative temperature may be of order 18°C, much lower than used by Toole and Warren (1993). Detailed justification for these adjustments is now presented.

Year-long current meter measurements were made on 5 moorings deployed across the Agulhas Current from February 1995 to April 1996 (Bryden et al., 1995). Record-length average velocities have been estimated for each of the instruments and the alongslope (220°T) velocities (Fig. 3) have been integrated vertically from 2400 m depth to the surface and horizontally from the coast across the current out to 203 km offshore to yield a net poleward transport of 70.3 Sv. Linear interpolation is used vertically between the current meters on each mooring generally sited at depths of 400, 800, 1200 and 2000 m. On the two moorings closest to the coast, acoustic Doppler current profilers measured velocity up to within 50 m of the sea surface. Velocity profiles are linearly extrapolated above the shallowest measurement level to the surface and below the 2000 m instrument level to 2400 m depth. Linear interpolation is also used horizontally where zero velocity is assumed on the continental slope and at 203 km. To establish the offshore boundary of the poleward flowing Agulhas Current, the time-averaged velocities on moorings E and F are extrapolated offshore at 400, 800 and 1200 m depths to determine the location of zero velocity. At each depth, zero velocity occurs at a distance of 45–56 km beyond mooring F, that is at offshore distances between 198 and

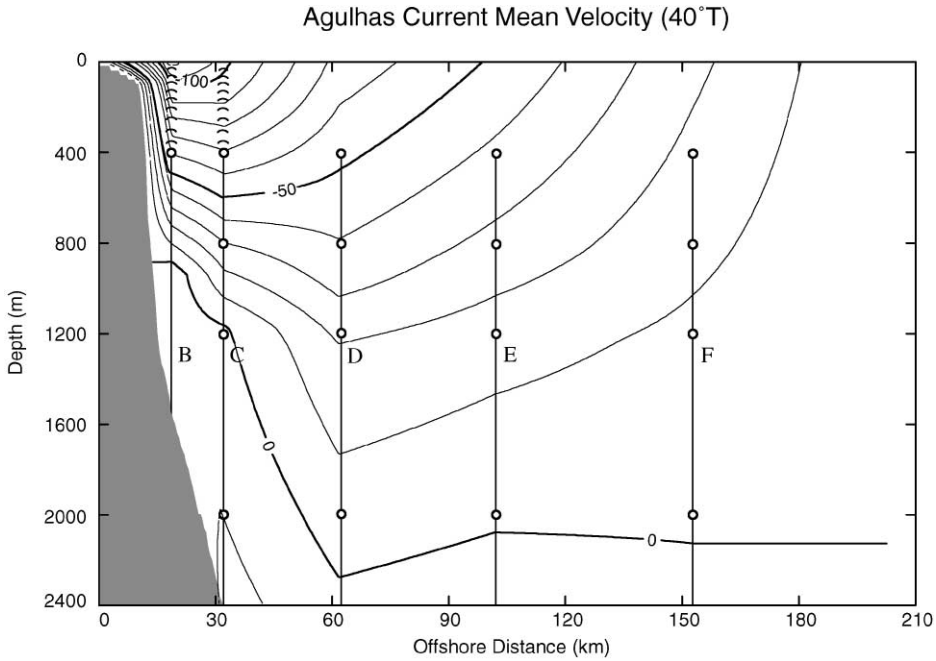

Fig. 3. Contoured velocity section across the Agulhas Current derived from time-averaged currents measured by the year-long array of moored current meters deployed from February 1995 to April 1996. The array extends southeast from Port Edward, South Africa along the section of Discovery CTD stations shown in Fig. 1. The contoured velocity at 10 cm s^{-1} intervals is the component directed alongshore toward 40°T, so that negative velocities are poleward. The depth of the zero-velocity contour is used as the reference level for geostrophic calculations of Agulhas Current transport for *Discovery* stations out to station 15.

209 km. The average position for zero velocity of 203 km is then taken to represent the offshore boundary of the poleward flow of the Agulhas Current.

The contoured mean velocity section (Fig. 3) exhibits both the strong poleward flow of the Agulhas Current and the equatorward flow of the Agulhas Undercurrent hugging the continental slope. The zero-velocity surface for the mean currents intersects the continental slope at about 900 m depth and then trends downward offshore. In the offshore region beyond 60 km from the coast there is a zero-velocity surface for the mean currents at about 2200 m, in contrast to the V-shaped zero-velocity surface observed in the synoptic LADCP section in February–March 1995 (Beal and Bryden, 1997). A time series of Agulhas transport has also been developed for the 267-day period of reasonably complete instrument coverage by assigning an area to each available current meter. The mean transport for this 267-day period is 69.7 Sv with a standard deviation for daily averaged transports of 21.5 Sv. The synoptic transport based on the current meter measurements during the period in early March when the 1995 CTD/LADCP section was taken is 73.1, or 3.4 Sv larger than the mean transport. The congruence of the transports from the current meters, the LADCP section, and from the hydrographic section referenced to the synoptic LADCP measurements suggests that the average Agulhas Current transport is about 70 Sv.

Based on the observed structure and transport in the time-averaged Agulhas Current, the geostrophic transport for the western boundary portion of the joined 1995–1987 transindian hydrographic section is adjusted to have an integrated transport of 70 Sv between the surface and 2400 m depth and from the coast out to station D15 at a distance of 194 km from the coast: The initial zero-velocity surface for the geostrophic velocity profiles was taken directly from the structure of the zero-velocity surface in the mean velocity section (Fig. 3); then a barotropic, uniform velocity of 0.87 cm s^{-1} was added in this western boundary region to force the transport to be 70 Sv. For comparison with Toole and Warren's (1993) discussion of the Natal Valley transect out to station CD17 at the top of the Mozambique Plateau, we estimated the net poleward transport using the joined section to be 64.4 Sv, or 15.4 Sv less than Toole and Warren's net transport of 79.8 Sv. As noted by Toole and Warren (1993), the Natal Valley is a cul-de-sac below about 2750 m so that the net meridional flow below this depth should be small. Indeed, for the joined 1995–1987 section across the Natal Valley, the northward transport below 2800 dbar is 1.5 Sv and not much larger than the 0.8 Sv in Toole and Warren's analysis. In summary, there is 15 Sv less poleward flow in this present analysis based on direct current measurements compared to Toole and Warren's western boundary analysis.

The second adjustment is to the eastern boundary region off the coast of Australia where current meter measurements suggest that the poleward flowing Leeuwin Current is in fact a relatively shallow current overlying a substantial equatorward flow in the deeper waters (Domingues et al., 1999). The current meter measurements are admittedly at 22°S, but they suggest that the zero-velocity contour is in the depth range between 150 and 200 m, a marked change from the concept of a deep-reaching poleward flow in the Leeuwin Current. As a result of these measurements, we use a reference level of 160 dbar for station pairs beginning with station CD103 within 100 km of the Australian coast. Overall the meridional transport in this eastern boundary region changes from 2.7 Sv poleward with the Toole and Warren (1993) reference levels to 2.1 Sv equatorward with the shallower reference levels based on the current meter measurements, a net addition of 4.8 Sv to the equatorward transport.

The third adjustment is made over the Broken Plateau, which the 1987 transindian hydrographic section unfortunately traversed for 1200 km between 87 and 99°E. Use of the bottom as a reference level over Broken Plateau following Toole and Warren (1993) yields a net equatorward transport of only 0.6 Sv between stations CD69 and CD80, and such transport is substantially less than estimates of wind-driven Sverdrup transport would suggest over this longitude range. Three wind climatologies are examined for Sverdrup transport across 31–33°S between 85 and 100°E: Hellerman and Rosenstein (1983) yielded 10.7 Sv, the ECMWF winds used in OCCAM yielded 8.2 Sv (Saunders, personal communication) and the SOC climatology (Josey et al., 2001) yielded 6.9 Sv. Over the complete breadth of the 32°S section, Sverdrup transports were estimated to be 48 Sv (Hellerman and Rosenstein), 43 Sv (ECMWF) and 40 Sv (SOC), which are similar to the mid-ocean geostrophic transports referenced to zero velocity in the deep water shown in Table 1. In a study of the Pacific circulation in the OCCAM numerical model, Saunders et al. (1999) found remarkable agreement between the distribution of Sverdrup transport and the meridional mid-ocean flow in the model. To account for the anticipated Sverdrup transport, the net equatorward transport over Broken Plateau is forced to equal 5.5 Sv, the Sverdrup transport estimated from the SOC climatology for the section between 87 and 99°E, by adding a uniform bottom velocity of $0.33\,\mathrm{cm\,s^{-1}}$ everywhere between stations 69 and 80. The argument for such bottom velocity is that if the transindian section had been taken just a bit further north or south off the Plateau in deeper waters there would have been observed a small equatorward shear relative to zero velocity in the deeper waters that would have produced such a bottom velocity and associated Sverdrup transport. Overall, this adjustment over Broken Plateau increases the mid-ocean equatorward transport by 5 Sv.

The final consideration is the Indonesian Throughflow, which Toole and Warren (1993) estimated to be 6.7 Sv at an average temperature of 24°C. Recent measurements and estimates suggest that the Throughflow is larger and occurs at lower temperature. In particular, current meter measurements in Makassar Strait exhibit a transport of 9 Sv centred at about 300 m depth with an average temperature of about 12°C (Gordon et al., 1999; Ffield et al., 2000). Makassar Strait is only one of several straits so the overall Throughflow may well be larger and warmer. For the circulation estimates made here, we will use a baseline Throughflow transport of 12 Sv at an average temperature of 18°C, which are the values in the OCCAM simulation (Saunders et al., 1999), and then consider how the circulation would change for Throughflow variations of 5 Sv and 6°C about these values. The Throughflow transport in OCCAM corresponded to the island-rule value (Godfrey, 1989) for the ECMWF winds used in OCCAM.

Following these adjustments, the Toole and Warren (1993) circulation across 32°S has effectively been modified so that there is 15 Sv less poleward flow in the western boundary region; 4.7 Sv more equatorward flow in the eastern boundary region; 5 Sv more equatorward flow over Broken Plateau; and an increase in the Throughflow by 5.3 Sv. All of these adjustments serve to diminish the need for substantial, zonally averaged deep northward velocities across the 32°S section. These adjustment have changed the horizontal structure of the meridional flow across 32°S by about 30 Sv.

With these adjustments and with a mid-ocean zero-velocity surface at 2200 dbar, the net mass convergence into Indian Ocean north of the 32°S transindian section is $1.74\times10^{9}\,\mathrm{kg\,s^{-1}}$ and the salt convergence is $41.7\times10^{6}\,\mathrm{kg\,s^{-1}}$. To eliminate the salt convergence, a uniform barotropic velocity of $-0.0048\,\mathrm{cm\,s^{-1}}$ is added everywhere east of station CD15 at the offshore end of the

Agulhas Current. After this final adjustment, the mass convergence is $0.54 \times 10^9\,\mathrm{kg\,s^{-1}}$ which represents our estimate for the net evaporation over the Indian Ocean north of 32°S. Such convergence is slightly larger than Toole and Warren's (1993) estimate of $0.48 \times 10^9\,\mathrm{kg\,s^{-1}}$ or Robbins and Toole's (1997) estimate of $0.31 \times 10^9\,\mathrm{kg\,s^{-1}}$, but similar to the estimate of net evaporation for the Indian Ocean north of 32°S of $0.56 \times 10^9\,\mathrm{kg\,s^{-1}}$ by Baumgartner and Reichel (1975). For this final circulation, the heat transport divergence is 0.66 PW. Hence, the Indian Ocean north of 32°S is gaining heat from the atmosphere at the rate of $17\,\mathrm{W\,m^{-2}}$ and exporting warmer water across its southern boundary to create a heat transport divergence of 0.66 PW. Such heat transport divergence is smaller than Toole and Warren's estimate of 0.98 PW but larger than Robbins and Toole's estimate of 0.42 PW, and similar to Bunker's estimate of 0.59 PW for the heat gained by the Indian Ocean north of 32°S from the atmosphere as reported by Talley (1984). Finally, for this circulation, the silica convergence is only $335\,\mathrm{kmol\,s^{-1}}$, so the Indian Ocean silica imbalance here is a factor of 5 less severe than the $1530\,\mathrm{kmol\,s^{-1}}$ in the Toole and Warren circulation as reported by Robbins and Toole.

The final diagnosed circulation across 32°S after all adjustments have been made consists of a southward Agulhas Current transport of 71.9 Sv overlying a northward Agulhas Undercurrent transport of 5.4 Sv for a net transport of 66.5 Sv in the western boundary region west of station D15 and a 52.9 Sv northward flow in the mid-ocean region east of station D15. The zonally averaged mid-ocean northward transport essentially extends throughout the water column except for a small net southward flow of 1.5 Sv between 1500 and 2400 dbar. Such southward flow may be indicative of a return path for northward flowing deep and bottom waters entering the Indian Ocean across 32°S. In terms of the vertical–meridional circulation, the overturning is much less than in the Toole and Warren (1993) circulation. There is a net equatorward transport in the waters below 2000 dbar of 10.1 Sv, where 4.3 Sv is contributed by the northward flow beneath the Agulhas Current and 5.8 Sv occurs in the mid-ocean region east of station D15. Such overturning is less even than in Robbins and Toole's (1997) circulation constrained to conserve silica.

7. Mechanisms of heat and freshwater transports

For understanding what processes lead to the overall heat transport it can be helpful to separate the fluxes into components. Here we follow and develop the separation into components used by Roemmich and Wunsch (1985), Bryden et al. (1991), Saunders and Thompson (1993) and Bryden (1993).[6] First we separate meridional velocity, v, and potential temperature, Θ into section-averaged values, $\langle \bar{v} \rangle$ and $\langle \underline{\bar{\Theta}} \rangle$, zonally averaged baroclinic values, $\langle v \rangle(z)$ and $\langle \Theta \rangle(z)$, and deviations from zonal averages, $v'(x,z)$ and $\Theta'(x,z)$, where

$$v = \langle \underline{\bar{v}} \rangle + \langle v \rangle(z) + v'(x,z) \text{ and } \Theta = \langle \underline{\bar{\Theta}} \rangle + \langle \Theta \rangle(z) + \Theta'(x,z).$$

[6] It is worthwhile to note that we do not follow the component separation used by Bryden and Hall (1980) and Hall and Bryden (1982) because we find that such separation, while potentially helpful in terms of calculation procedures, does not aid our physical understanding of the mechanisms of heat transport.

Then the geostrophic component of the heat transport can be broken up into 3 parts (Table 3):

1. A barotropic part due to the net transport across the 32°S section at the section-averaged temperature of 4.70°C

$$\rho C_p \langle \underline{\bar{v}} \rangle \langle \underline{\bar{\Theta}} \rangle \int L(z)\,dz,$$

where ρ is density, C_p is specific heat of seawater, $L(z)$ is the width of the section at each depth and $\int L(z)\,dz$ is the area of the section;

2. A baroclinic heat flux due to the zonally averaged geostrophic vertical–meridional circulation

$$\int \rho C_p \langle v \rangle(z) \langle \Theta \rangle(z) L(z)\,dz$$

in which warm surface waters flow southward and cold deep waters flow equatorward across 32°S with no overall mass transport;

3. A horizontal heat flux due to the large-scale gyre circulation

$$\int dz \int dx \rho C_p v' \Theta'$$

in which at each depth colder waters flow northward over the mid-ocean region and return southward at warmer temperatures in the Agulhas Current but with no net mass transport at any depth.

Table 3
Heat transport across 32°S[a]

Component	Mass transport (10^9 kg s^{-1})	θ (°C)	S	Temperature transport (PW)	Salt transport (10^6 kg s^{-1})
(a) Fluxes associated with net flows across boundaries					
Barotropic Geostrophic	− 13.42	4.70	34.76	− 0.249	− 466.5
Indonesian Throughflow	12.31	18	34.5	0.884	424.7
Surface Ekman	1.65	19.58	35.66	0.129	58.8
Net evaporation	− 0.54	28	0.0	− 0.063	0
Net Barotropic heat and salt fluxes	0.00			+ 0.701	+ 17.0

	Mass transport (10^9 kg s^{-1})	Heat transport (PW)	Salt transport (10^6 kg s^{-1})
(b) Components of meridional heat transport			
Net barotropic flux	0	0.701	17.0
Baroclinic flux	0	− 0.618	− 3.0
Horizontal flux	0	− 0.746	− 14.0
Overall heat and salt transports		− 0.663	0

[a]Positive values represent fluxes into the Indian Ocean bounded on the south by the 32°S section, on the northeast by the Indonesian passages, and by the sea surface.

Because they conserve mass by definition, the baroclinic and horizontal heat fluxes contribute directly to the meridional ocean heat transport. Because it includes a net mass transport, the barotropic–geostrophic component must be combined with other components that include a mass transport across the boundaries such as the Throughflow, Ekman transport, and net evaporation to determine a barotropic heat flux with mass conserved before it can be directly added to the meridional heat transport (Table 3).

The baroclinic heat flux and horizontal heat flux each contribute poleward heat transports comparable to the overall heat flux divergence (Table 3). The baroclinic heat flux of -0.62 PW (negative values represent divergent or southward fluxes) is associated with the cold water to warm water conversion process in the Indian Ocean which is often linked to the global Conveyor Belt: a net northward flow of 10.1 Sv of cold, deep water enters the Indian Ocean from the south below 2000 dbar and must be warmed up before exiting the Indian Ocean above 2000 dbar. The horizontal heat flux of -0.75 PW is associated with the anticyclonic subtropical gyre circulation which typically includes mid-ocean equatorward flow and a warm, poleward flowing western boundary current. It is relatively easy to understand the heat flux associated with the horizontal circulation as heat gained from the atmosphere warms the equatorward flowing waters which then circulate and leave the basin in a warm western boundary current. Such horizontal heat flux is closely related to the size of the Agulhas Current. Because the Agulhas Current is approximately 2°C warmer overall than the mid-ocean section, a 70 Sv Agulhas Current accounts for most of the horizontal heat flux across 32°S. It is more difficult to understand the baroclinic heat transport because it involves a conversion of cold deep water into warmer intermediate and upper deep waters. Identifying the processes that mix the heat downward to warm the cold deep water continues to be a puzzle that clouds the interpretation of the baroclinic heat flux. For example, Toole and Warren (1993) argued for enhanced diapycnal mixing perhaps due to rougher bottom topography in the Indian Ocean than in other oceans.

Combining the net barotropic geostrophic flow across 32°S with the Ekman, Throughflow, and net evaporation mass fluxes across the boundaries results in a net convergence of heat into the Indian Ocean north of 32°S of 0.70 PW (Table 3). This component is due to both the Throughflow and the wind-driven Ekman transports contributing warm waters to the Indian Ocean which must cool before exiting across the southern boundary. There is also a small effect on the heat budget due to the mass flux leaving the surface of the Indian Ocean as a result of evaporation. Under the assumption that the 0.54×10^9 kg s^{-1} of net evaporation leaves the ocean surface at a temperature of 28°C, the resultant heat loss is 0.06 PW. Thus, the warmth of the Throughflow and Ekman transports contributes along with air–sea heat exchange to the overall warming of the Indian Ocean waters. Their heat contributions can be readily understood to warm the upper-level, horizontal circulation of the subtropical gyre. The processes by which the heat gain from the atmosphere and the warmth associated with the Ekman and Throughflow transports can be mixed downward to raise the temperature of the northward flowing cold deep waters so that they can return southward at warmer temperatures and shallower depths are unclear.

In a similar manner as for heat, the barotropic, baroclinic, and horizontal salinity fluxes can be quantified (Table 3). The combined contribution to the salinity (or freshwater) flux from the barotropic geostrophic flow across 32°S and the Throughflow, Ekman and net evaporation suggests that the net transport out of the region is fresher than the net transport into the region by 17×10^6 kg (salt) s^{-1} [1 Sv ppt is approximately equal to 1×10^6 kg s^{-1} of salt transport]. This

barotropic component is effectively due to the net evaporation of $0.54 \times 10^9\,\mathrm{kg\,s^{-1}}$ leaving the ocean at a salinity of 0, or about 35 less than the typical ocean salinity of the inflowing waters. To conserve salt for the region, the combined baroclinic and horizontal salinity fluxes must remove $17 \times 10^6\,\mathrm{kg\,s^{-1}}$ of salt southward across 32°S. The baroclinic salinity transport is relatively small, $-3 \times 10^6\,\mathrm{kg\,s^{-1}}$, because there is little vertical salinity gradient in the zonally averaged properties across 32°S. Thus, the horizontal salinity flux across 32°S of $-14 \times 10^6\,\mathrm{kg\,s^{-1}}$ provides the principal salinity export representing more than 80% of the total salinity transport required to maintain the salt budget for the Indian Ocean in the presence of the net evaporation. Again, the Agulhas is largely responsible as it is of order 0.2 saltier than the mid-ocean section. The subtropical gyre circulation of 70 Sv of fresher waters flowing northward across the interior Indian Ocean and returning southward in the Agulhas Current at higher salinity generates three-quarters of the required salinity (or freshwater) transport across 32°S.

The vertical distributions of the horizontal heat and salt transports across 32°S (Fig. 4) show that substantial contributions are made by the circulation all the way down to 1500 dbar in the Indian Ocean. In terms of mechanisms then, at each depth relatively colder and fresher waters flow

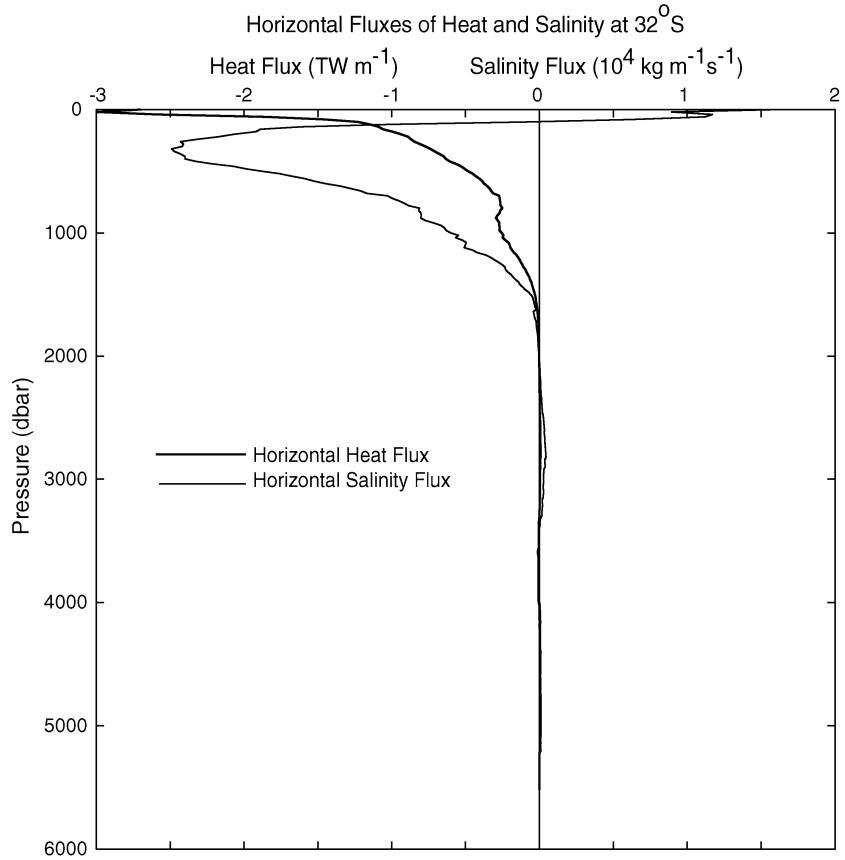

Fig. 4. Vertical profiles of horizontal heat and salinity fluxes across 32°S in the Indian Ocean. Negative values indicate poleward (southward) fluxes.

northward across the interior 32°S section, they gain heat and salt due to the overall heat gain and net evaporation over the Indian Ocean and hence return southward primarily in the Agulhas Current as warmer and saltier waters. The penetration of these horizontal fluxes to depths as great as 1500 m surprised us.

8. Discussion

In starting this study, we had anticipated from Toole and Warren's (1993) results that most of the poleward heat transport in the Indian Ocean was carried by the large meridional overturning circulation that they had estimated to consist of a 27 Sv northward flow of cold waters below 2000 dbar with a compensating southward flow of warmer waters above 2000 dbar. Reducing the size of this vertical–meridional circulation should then proportionately reduce the size of the heat flux. In deriving this new circulation, we now estimate that the overturning circulation is reduced to 10.1 Sv, a reduction of 63% compared to Toole and Warren's overturning. The heat flux divergence, however, is reduced by only 32% from Toole and Warren's value. In point of fact, as shown by the similarity in solutions for different reference levels in Table 1, the baroclinic structure of the mid-ocean geostrophic circulation is insensitive to the size of the overturning indicated by the net northward flow below 2000 dbar. In the absence of changes to the large-scale baroclinic structure then, the baroclinic heat and freshwater fluxes are nearly constant and the overall heat and freshwater fluxes vary primarily with the size of the horizontal circulation, that is with the size of the western boundary current which is warmer and saltier than the interior circulation.

The penetration of the horizontal heat and salinity fluxes down to depths of 1500 m suggests to us that Red Sea water formation is fundamentally involved in the conversion process of turning cold deep water into warmer intermediate and upper deep waters. Making Red Sea water is a buoyancy loss process that involves a heat loss and a salinity gain with the salinity increase dominating the increase in density. At Bab el Mandab, the southern exit of the Red Sea, the outflow of about 0.4 Sv has a temperature of 22°C and a salinity of 40 (Murray and Johns, 1997). After flowing over the sill, some of the Red Sea Water plunges down into the deep Gulf of Aden: water at 1400 m depth has been observed to have temperatures above 15°C and to be saltier than 37 both historically (Wyrtki, 1971) and on the 1995 WOCE I1 hydrographic section when waters with potential temperature of 16.5°C and salinity of 37.64 were observed at 1450 m depth (Morrison, personal communication). Outside the Gulf of Aden, the principal Red Sea water influence spreads out initially between 600 and 800 m as a salinity maximum which then appears to descend slowly to 1200 m depth before it fades out near 20°S (Wyrtki, 1971), though Beal et al. (2000) find traces of Red Sea water extend farther southwards principally along the western boundary. As well as being a source of heat and salinity for the intermediate and upper deep water layers, such a warm, salty water mass relative to the waters beneath can also lead to further downward heat and salt fluxes associated with the salt fingering process. It is possibly the double diffusive effects associated with warm, salty Red Sea water that lead to the higher diapycnal diffusivities for the Indian Ocean that are needed to make the deep waters warmer and saltier.

The Red Sea water formation process suggests a reassessment of the standard concept of the Indian Ocean as a region of net buoyancy gain. Could the Indian Ocean actually be a region of net buoyancy loss due to the high evaporation? Overall, we estimate that the Indian Ocean north of

32°S gains 0.66 PW of heat from the atmosphere (HF) and loses freshwater due to net evaporation (E) of 0.54×10^9 kg s^{-1}. To determine the relative effects of the heat flux and net evaporation on the buoyancy

$$d\rho = \frac{\partial \rho}{\partial T} dT + \frac{\partial \rho}{\partial S} dS = -\alpha dT + \beta dS,$$

where $dT = HF/\rho C_p$ and $dS = ES/\rho$, we use expansion coefficients, $\alpha = 3.1 \times 10^{-4}$ gm cm^{-3} °C^{-1} and $\beta = 7.2 \times 10^{-4}$ gm cm^{-3} ppt^{-1}, for a typical surface temperature of 28°C and salinity of 35.5. The heat flux contributes a buoyancy gain of $\alpha HF/\rho C_p$ equal to 5.0×10^{10} gm and the net evaporation contributes a buoyancy loss of $\beta ES/\rho$ of 1.3×10^{10} gm. Thus the buoyancy gain due to the heat loss is a factor of 4 larger than the buoyancy loss due to net evaporation. Even for the smaller heat gain of 0.43 PW estimated by Robbins and Toole (1997) for their circulation constrained to conserve silica, the buoyancy gain due to the air–sea heat exchange would be a factor of 2.5 larger than the buoyancy loss due to the net evaporation. We conclude that the Indian Ocean north of 32°S is indeed a region of net buoyancy gain despite high net evaporation. Nevertheless, buoyancy loss due to large evaporation can dominate in certain regions like the Red Sea and the resulting dense water formation in these small regions can transmit heat (and salt) downward into the deep interior ocean.

After the direct current measurements have established the structure and transport of the Agulhas Current, the major uncertainties in diagnosing the overall circulation and heat flux in the Indian Ocean are the size of the Indonesian Throughflow and its associated temperature and salinity characteristics. There seems to be general agreement that the Throughflow has a salinity of about 34.5. Here, we have taken model-based values of 12 Sv and 18°C for the Throughflow transport and transport-weighted temperature. Previous estimates of the Throughflow transport have suggested that 7 Sv is a representative annual average at a temperature as high as 24°C (Wijffels et al., 1996), while new current meter measurements in only one of the passages indicate a transport of 9.3 Sv ± 2.5 Sv (Gordon et al., 1999) at a temperature of less than 12°C (Ffield et al., 2000). To estimate uncertainties in the fluxes, we assume the 12 Sv Throughflow transport has an uncertainty of 5 Sv and its 18°C temperature has an uncertainty of 6°C. Based on the sensitivity studies reported above, a 5 Sv uncertainty in Throughflow transport corresponds to an uncertainty in heat flux divergence over the Indian Ocean of 0.40 PW and to an uncertainty in net evaporation of 0.04×10^9 kg s^{-1}. Because a 5 Sv change in the Throughflow transport would change the silica convergence by 375 kmol s^{-1}, more than enough to eliminate the silica convergence in the circulation presented above, we have not tried to force the silica convergence toward zero as Robbins and Toole (1997) did. In fact, we would argue that a 5 Sv uncertainty in Throughflow transport means that the uncertainty on silica convergence is at least ± 400 kmol s^{-1}. From Table 3, we can estimate that the uncertainty in Throughflow temperature of 6°C for constant transport of 12 Sv would lead to an uncertainty in heat flux divergence over the Indian Ocean of 0.29 PW, again a substantial error in heat flux. Clearly, the uncertainties on the Throughflow transport and its associated temperature must be reduced before reliable comparisons can be made between heat transport divergence over the Indian Ocean and the air–sea heat exchange in climatologies that are used to force numerical models of ocean circulation.

There has been great emphasis on the meridional overturning circulation in the Indian Ocean since Toole and Warren (1993) described the large overturning resulting from their analysis of the

1987 transindian hydrographic section. Models have tried to reproduce the large overturning circulation (Lee and Marotzke, 1997; Banks, 2000) and arguments persist over how large the overturning is and what processes are necessary to sustain it (Robbins and Toole, 1997; Macdonald, 1998; Ganachaud et al., 2000). We stress here that the circulation across 32°S is much more than a single number related to the overturning: there is a substantial horizontal gyre circulation, a factor of 5 larger than the overturning, in which there is a strong poleward flow of warm and salty waters in the western boundary current and a broad equatorward flow of colder and fresher waters over the mid-ocean expanse of the Indian Ocean (Fig. 5); and there are several deep western boundary currents as well as the Agulhas Undercurrent carrying cold deep waters northward across 32°S and the return pathways for these cold deep waters are likely to be complex. In vertical coordinates (Fig. 5a), the southward Agulhas Current transport in the upper 1000 dbar of 62.1 Sv is largely compensated by the northward mid-ocean transport in the upper 1000 dbar of 44.5 Sv plus the net evaporation, Ekman and Throughflow transports of 13.1 Sv. From 1000 to 2000 dbar, the southward Agulhas transport of 8.7 Sv is partially balanced by 3.1 Sv of net northward flow in the mid-ocean region. The relatively small differences between these horizontal transports, 4.5 Sv in the upper 1000 dbar and 5.6 Sv between 1000 and 2000 dbar, represents the upper limb of the meridional overturning circulation. There is undoubtedly horizontal structure to the deep water circulation as well and the net northward transport of cold deep waters may be a relatively small

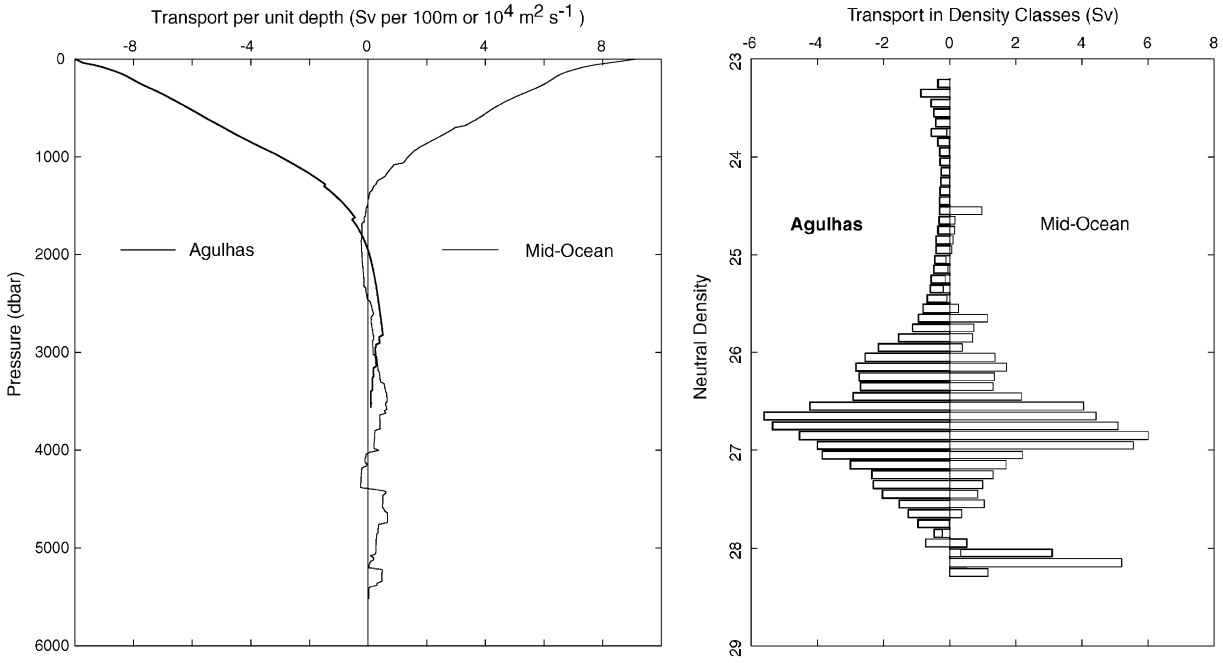

Fig. 5. Vertical structure of the meridional circulation across 32°S in the Indian Ocean (a) in vertical (pressure) coordinates and (b) in density coordinates. Transport per unit depth equals the zonally averaged cross-track (positive northward) velocity multiplied by the effective width at each pressure level. Transport in Sverdrups is given for neutral density intervals of 0.1. The width of the Agulhas western boundary region is 195 km while the width of the mid-ocean expanse of the Indian Ocean section beyond *Discovery* station 15 is 8040 km.

difference between fast, northward flowing deep western boundary currents and broad, slow, southward flowing mid-ocean currents. In density coordinates (Fig. 5b), there is a clear southward transport of upper, low density (neutral density less than 25.5) waters in the Agulhas associated with the Throughflow, a large circulation of order 50 Sv northward in mid-ocean and 50 Sv southward in the Agulhas in the neutral density interval between 25.5 and 27.7, and a northward transport of the densest deep waters. The overall meridional overturning in density consists of a northward transport of 10.3 Sv in the densest waters (neutral density greater than 28.0) with 3.6 Sv beneath the Agulhas and 6.7 Sv over the mid-ocean region that is effectively balanced by a net southward flow of 9.7 Sv for densities between 27.0 and 28.0. This compensating net southward flow, however, is small compared with the size of the gyre circulation. In summary, the meridional overturning circulation in the Indian Ocean is a small residual of a vigorous horizontal circulation in the upper waters and undoubtedly in the deeper waters as well.

With respect to the size of the overturning circulation in the Indian Ocean, we have shown how direct current measurements in the western and eastern boundary regions constrain the size of the overturning circulation diagnosed from long hydrographic sections. Further constraints may be derived in the future from direct current measurements across mid-ocean regions. Analysis of long-term current meter measurements made during WOCE in the deep western boundary currents may quantify how much cold deep water is flowing northward. For the vast mid-ocean regions, new current measurement techniques using lowered acoustic Doppler current profiles and neutrally buoyant floats have been introduced and underway acoustic current profiling has improved dramatically (King et al., 2001) since the 32°S transindian hydrographic section was done in 1987. Such measurement techniques on a transindian transect may help to delineate the horizontal structure of the circulation in the upper waters and the return pathways of the cold deep waters and hence to define the structure and size of the overturning circulation.

Acknowledgements

The CTD-LADCP sections across the Agulhas Current in 1995 aboard RRS *Discovery* and in 1996 aboard R.V. *Algoa* and the year-long current meter measurements were supported by the Natural Environment Research Council (NERC) under the UK WOCE Community Research Programme. We thank the South African Sea Fisheries Research Institute for arranging shiptime on R.V. *Algoa*. NERC also generously supported the analysis reported here by the first author under the Core Strategic Research Project "Observing and Modelling Seasonal to Decadal Variability in the Ocean" and by the second author under a WOCE Special Topic studentship at the University of Southampton. Further analysis by the second author was supported by the National Science Foundation under grants OCE97-29322 and OCE99-07458. We thank Paul Robbins for providing the details of earlier calculation procedures used on the 32°S section.

References

Banks, H.T., 2000. Indonesian Throughflow in a coupled climate model and the sensitivity of the heat budget and deep overturning. Journal of Geophysical Research 105, 26135–26150.

Baumgartner, A., Reichel, E., 1975. The World Water Balance. Elsevier, New York, 179p.
Beal, L.M., 1997. Observations of the velocity structure of the Agulhas Current. Ph.D. Thesis, Department of Oceanography, University of Southampton, 158 p.
Beal, L.M., Bryden, H.L., 1997. Observations of an Agulhas Undercurrent. Deep-Sea Research I 44 (9–10), 1715–1724.
Beal, L.M., Bryden, H.L., 1999. The velocity and vorticity structure of the Agulhas Current at 32°S. Journal of Geophysical Research 104, 5151–5176.
Beal, L.M., Ffield, A., Gordon, A.L., 2000. Spreading of Red Sea overflow waters in the Indian Ocean. Journal of Geophysical Research 105, 8549–8564.
Bryan, K., 1962. Measurements of meridional heat transport by ocean currents. Journal of Geophysical Research 67, 3403–3414.
Bryden, H. L., 1993. Ocean heat transport across 24°N latitude. In: McBean, G.A., Hantel, M. (Eds.), Interactions Between Global Climate Subsystems: The Legacy of Hann, Geophysical Monograph, Vol. 75, pp. 65–75.
Bryden, H.L. et al., 1995. RRS Discovery cruise 214, 26 Feb–09 Mar 1995: Agulhas Current Experiment. Cruise Report 249, Institute of Oceanographic Sciences. Wormley, 85p.
Bryden, H.L., Hall, M.M., 1980. Heat transport by currents across 25°N latitude in the Atlantic Ocean. Science 207, 884–886.
Bryden, H.L., Roemmich, D.H., Church, J.A., 1991. Ocean heat transport across 24°N in the Pacific. Deep-Sea Research 38 (3A), 297–324.
Domingues, C.M., Wijffels, S., Tomczak, M., Church, J.A., 1999. Volume transports and structure of the Leeuwin Current at 22°S-WOCE ICM6. International WOCE Newsletter 37, 36–40.
Donohue, K.A., Firing, E., Beal, L.M., 2000. Comparison of three velocity sections of the Agulhas Current and Undercurrent. Journal of Geophysical Research 105, 28585–28594.
Ffield, A., Vranes, K., Gordon, A.L., Susanto, R.D., 2000. Temperature variability within Makassar Strait. Geophysical Research Letters 27, 237–240.
Ganachaud, A., Wunsch, C., Marotzke, J., Toole, J., 2000. Meridional overturning and large-scale circulation of the Indian Ocean. Journal of Geophysical Research 105, 26117–26134.
Godfrey, J.S., 1989. A Sverdrup model for the depth-integrated flow for the world ocean allowing for island circulations. Geophysical and Astrophysical Fluid Dynamics 45, 89–112.
Gordon, A.L., Susanto, R.D., Ffield, A., 1999. Throughflow within Makassar Strait. Geophysical Research Letters 26, 3325–3328.
Hall, M.M., Bryden, H.L., 1982. Direct estimates and mechanisms of ocean heat transport. Deep-Sea Research 29 (3A), 339–359.
Hellerman, S., Rosenstein, M., 1983. Normal monthly wind stress over the world ocean with error estimates. Journal of Physical Oceanography 13, 1093–1104.
Josey, S.A., Kent, E.C., Taylor, P.K., 2001. On the wind stress forcing of the ocean in the SOC and Hellerman and Rosenstein climatologies. Journal of Physical Oceanography, submitted.
King, B.A., Firing, E., Joyce, T., 2001. Shipboard observations during WOCE. In: Church, J., Gould, J., Siedler, G. (Eds.), Ocean Circulation and Climate. Academic Press, New York, pp. 99–122.
Lee, T., Marotzke, J., 1997. Inferring meridional mass and heat transports of the Indian Ocean by fitting a general circulation model to climatological data. Journal of Geophysical Research 102, 10585–10602.
Macdonald, A.M., 1998. The global ocean circulation: a hydrographic estimate and regional analysis. Progress in Oceanography 41, 281–382.
Murray, S.P., Johns, W., 1997. Direct observations of seasonal exchange through the Bab el Mandab Strait. Geophysical Research Letters 24, 2557–2560.
Robbins, P.E., Toole, J.M., 1997. The dissolved silica budget as a constraint on the meridional overturning circulation of the Indian Ocean. Deep-Sea Research I 44 (5), 879–906.
Roemmich, S., Wunsch, C., 1985. Two transatlantic sections: meridional circulation and heat flux in the subtropical North Atlantic Ocean. Deep-Sea Research 32 (6), 619–664.
Saunders, P.M., Coward, A.C., de Cuevas, B.A., 1999. Circulation of the Pacific Ocean seen in a global ocean model: Ocean Circulation and Climate Advance Modelling project (OCCAM). Journal of Geophysical Research 104, 18281–18299.

Saunders, P.M., Thompson, S.R., 1993. Transport, heat, and freshwater fluxes within a diagnostic numerical model (FRAM). Journal of Physical Oceanography 23, 452–464.

Talley, L.D., 1984. Meridional heat transport in the Pacific Ocean. Journal of Physical Oceanography 14, 231–241.

Toole, J.M., Warren, B.A., 1993. A hydrographic section across the subtropical South Indian Ocean. Deep-Sea Research I 40 (10), 1973–2019.

Wijffels, S.E., Bray, N., Hautala, S., Meyers, G., Morawitz, W.M.L., 1996. The WOCE Indonesian Throughflow repeat hydrography sections: I10 and IR6. International WOCE Newsletter 24, 25–28.

Wyrtki, K., 1971. Oceanographic Atlas of the International Indian Ocean Expedition. Superintendent of Documents, U.S. Government Printing Office, Washington, DC, 531 p.